Estimation of gas induction in jet loop reactors: Influence of nozzle designs

Sharma, D. V., Patwardhan, A. W., & Ranade, V. V. (2017). Estimation of gas induction in jet loop reactors: Influence of nozzle designs. DOI: 10.1016/j.cherd.2017.06.027

Published in:
Chemical Engineering Research and Design

Document Version:
Peer reviewed version

Estimation of Gas Induction in Jet Loop Reactors:
Influence of Nozzle Designs

Deepankar V Sharma[1,2], Ashwin W Patwardhan[2] and Vivek V Ranade[1,3*]

[1]Chemical Engineering and Process Development Division
CSIR - National Chemical Laboratory
Pune 411008, India

[2]Department of Chemical Engineering
Institute of Chemical Technology
Mumbai 400019, India

[3]School of Chemistry and Chemical Engineering
Queen's University Belfast, Belfast, NI, UK
[V.Ranade@qub.ac.uk]

* Author to whom correspondence should be addressed

Abstract:

Jet loop reactors are used widely for conducting gas liquid reactions because of the high mass transfer achieved in the gas-liquid ejector. Studies have shown that the mass transfer has a very strong correlation to the amount of gas induced in the ejector, and hence it is important to understand gas induction to enhance the performance of any gas-liquid nozzle. In this work, we used a single phase CFD model of the ejector with one adjustable parameter for estimating gas induction rates. After establishing that the model adequately describes the experimental data, the model was used for a quick evaluation of ejector geometries. Influence of key geometric parameters of gas-liquid ejectors like nozzle diameter, mixing tube length, distance between the nozzle outlet and mixing tube, suction chamber geometry and diffuser angle was investigated. It was found that dependence of gas induction on geometric parameters like distance between nozzle - mixing tube, suction chamber geometry, diffuser angle was either weak or had a clear maxima at or beyond a certain value of the geometric parameter. Other parameters like mixing tube length and nozzle diameter have a more complex impact on gas induction. The presented approach and results will be useful for quantifying influence of nozzle designs on gas induction rate in jet loop reactors.

Keywords: *Jet loop reactors, Gas induction, Nozzle geometry, CFD*

1. Introduction

Jet loop reactors (JLR) are extensively used in the industry as a gas-liquid contactor. Jet loop reactors are simple in design and find numerous applications in dead-end operations especially for processes like hydrogenation and chlorination [1]. The reason behind this is the intense mixing created in the gas liquid ejector which facilitates high mass transfer rates between gas and liquid. A external loop of a JLR consist of a hold up tank and a high powered pump which is used to maintain a high velocity jet in the ejector. The presence of external loop also facilitates removal of heat liberated during reactions via external heat exchanger. The designs on nozzle and ejector used in JLR are key factors in determining the overall performance. In this paper, we present results of experimental and computational studies on gas induction in JLR and influence of nozzle design on it.

In gas induction ejectors used in JLR, liquid is pumped through a nozzle creating a high velocity jet. The falling jet creates an envelope around it causing the surrounding gas to move along with the jet. If the velocity of this jet is increased the velocity of surrounding fluid also increases causing higher gas induction [2]. Any obstruction downstream of the jet like the throat of a venturi tube will adversely affect the fluid induction as more energy is required to overcome the pressure drop of the obstruction [3, 4, 5]. Thus the rate of gas induction is dependent upon the geometry of the ejector besides liquid flow rate. The mass transfer coefficient and gas hold up in the holdup tank also depend upon liquid flow rates and nozzle geometries. There are many published studies relating the gas hold up in the tank to gas induction and jet parameters like power of the nozzle [6, 7, 8]. Studies have shown that the mass transfer rates bear a close relation with gas induction rates hence it is imperative to study gas induction in ejectors for design and safe operation[9].

There have been many different experimental studies on gas induction in ejector and the major ones are listed in Table 1. While, some studies deal with up flow or side flow ejectors [10] used in bubble columns or aerators, most studies deal with down flow gas ejectors. Many different correlations were developed for correlating gas induction in ejectors [11, 12, 13]. These correlations correlate M_r or mass entrainment ratio to gas Euler number $\left(\Delta P_G / \rho_G u_G^2\right)$ or ratio of area of nozzle and throat (A_N / A_T). While the correlations have considerably different exponents and constants, the general theme of all the correlations is the same. Bhutada et al

[14] presents a very detailed experimentation on gas-liquid ejectors varying various different geometric parameters. Ben Brahim et al [15] shows a definite correlation for motive and entrained fluid Reynolds number for different motive and entrained fluids. All these studies are correlative in their approach and are reasonably successful in correlating the observed gas induction with the experimental parameters (Euler number) and fluid parameters [16].

There have been attempts to model the gas-liquid ejectors and jet loop reactors in general using lumped reaction engineering approach. In this approach, two phase plug flow models were developed for jet ejectors, and correlations were developed for hold up and mass transfer coefficient in the jet ejectors [17, 18, 9]. Similarly, tanks in series approach was developed for modeling jet loop reactor, in which the entire reactor including the recirculation loop was modelled as a network of reactor cells having gas-liquid, pure liquid and gas phase cells [19, 20]. These approaches work very well for specific system calculations but are not predictive and do not work as a design correlation/model.

To develop the model for prediction of gas induction, the study of flow characteristics of the jet is very important. Several efforts have been made to develop computational fluid dynamics (CFD) based models for simulating gas induction in gas –liquid ejector. Yadav et al, Kim et al and Yamoto et al have used the Eulerian – Eulerian (EE) and mixture model approach to model gas induction [21, 22, 23, 25]. Kandakure et al [24] have developed CFD methodology for estimating gas induction using the two phase mixture model framework. In the mixture model simulations algebraic expressions for slip velocity were used for modeling the interaction between gas and liquid instead for modeling the drag force between the phases. Notwithstanding some of the uncertainties associated with the mixture model, they have reported very good success in estimating gas induction.

The experimental studies have correlated different aspects of gas induction like gas inlet Reynolds number, gas Euler number to different jet parameters and jet Reynolds number [24]. The difference in the fitting parameters of the correlations reflect different ejector geometries. However, no explicit relationship between the different geometric parameters and gas induction was established. Even very detailed induction studies like Bhutada et al [3, 12, 14] develop separate correlations for different geometries instead of developing a single correlation using various geometric parameters. While all the experimental studies explain the driving force for induction as a suction force, no measurements of pressure was presented in the experimental data. Even for the calculations for gas Euler number there is no experimental

data provided. The reaction engineering models developed have too many unknowns like mass transfer coefficient, bubble diameter, gas hold up etc. Hence, correlative studies do not explain the phenomenon of gas induction and the impact of various geometric parameters on the same.

The simulations with the mixture model and the EE model either use algebraic slip or bubble diameter as an adjustable parameter to fit the simulated gas induction to experimental gas induction. While the simulated results show reasonable agreement with the experimental gas induction results, the simulation results show stratified flow in the jet ejector. This is contrary to the observations made while performing experiments. The published CFD studies have not covered the impact of various geometric parameters like design of diffuser section, or mixing tube length. In this work we have attempted to use simpler, single phase CFD model to simulate gas induction rate. The motivation behind this is that single phase simulations require order of magnitude lower computing resources and will allow quick evaluation of large number of nozzle configurations. This methodology assumes that as the driving force for the gas induction is the kinetic energy of the primary fluid or the power imparted by the nozzle, hence the mechanism of induction of a two phase gas-liquid ejector would be similar to the single liquid ejector. This work is focused on developing a CFD based methodology for estimating gas induction in nozzles used in jet loop reactors. The focus is on developing an approach which can be used to evaluate influence of various geometric parameters. The specific objectives are as following: development of a methodology and model for estimating gas induction rates as a function of liquid flow rate based on nozzle geometry and quantify the impact of various geometric parameter on gas induction in a jet ejector nozzle. Influence of geometric parameters of ejector were analyzed for developing a better understanding of significance and sensitivity of the various parameters. The presented approach and results will be useful for designing improved ejector configurations.

2. Experimental set up and methodology

The schematic of the experimental set up is shown in Figure 1a. The set-up consists of a holding tank, 5 hp centrifugal pump which pumps the primary/motive fluid/water into the jet ejector, jet ejector and associated flow and pressure measurement accessories. The details of jet ejector are shown in Figure 1b. The primary fluid (liquid) enters from the top nozzle and the secondary/entrained fluid (air) enter the suction chamber inlet. Both primary & secondary fluids mix in the mixing tube and become a two phase mixture. This two phase mixture then flows out of the ejector into the holdup tank which acts similar to a bubble column enhancing

the gas-liquid contact. In the holdup tank the gas and liquid mix vigorously due to the kinetic energy of the falling two phase jet. The gas rises upwards and exits from the tank. The liquid flows back into the recirculation tank completing the loop. The liquid flow rate was controlled by the rotameter shown in the Figure 1a.

Measurements of pressure drop across the gas liquid ejectors were taken by adding a pressure gauge just before the nozzle inlet. Since the outlet is open to atmosphere the outlet pressure of the nozzle is atmospheric pressure. In order to test the effect of the venturi nozzle part of ejector on the pressure drop of the ejector, two sets of experimental readings were taken for liquid nozzle diameter 8 and 10 mm. First without the ejector and second with the ejector. The measured pressure drop values for with and without the venturi part of the nozzle were almost the same (see Figure 2a).

The measurements of gas induction through the gas inlet were done using an anemometer Testo 416, provided and calibrated by Testo India Pvt. Ltd. with an accuracy of $\pm$ 6 x 10^{-6} m^3/s. The probe was attached at the gas inlet for measurement of gas induction by measuring the velocity of gas entering through the gas inlet. Precautions were taken so that no air came into the induction stream except for air coming into via the fan. For each measurement of gas induction three values were recorded, first being the time averaged velocity, second and third being the maximum and minimum velocity recorded in the specific time interval. The reported correlations were used to predict the gas induction results as seen in Figure 2b. The problem with these correlations, as seen in Table 1, that they do not correlate any geometric parameter to gas induction and only correlate the experimental data with various system variables like gas Euler number which was not measured. It can be seen that agreement between the values estimated from the correlations and experimental data is not so good.

3. Computational Model

3.1 Approach

As seen in Figure 2a, the pressure drop in the venturi part of the nozzle is insignificant as compared to the pressure drop of the liquid nozzle. This implies that the power imparted by the nozzle $\left(\Delta P_N Q_L\right)$ which is the driving force behind the gas-induction will not change because of the geometry of the venturi section. Furthermore, the frictional losses in the venturi section of ejectors have a very strong dependence on gas induction in an ejector and act as a counter balance to the driving force. Earlier modelling efforts using the EE or mixture models did not

capture the gas-liquid dispersion in the ejector and simulated stratified flow. Contrary to these results, the experiments showed excellent mixing of gas and liquid in the ejector. In order to ensure mixing of primary and entrained fluids in the ejector, here we decided to treat the entrained fluid as a miscible fluid with the primary fluid. This will ensure complete mixing of primary and entrained fluids in the ejector. The use of miscible fluids of course completely ignores interphase drag. In order to mimic interphase drag exhibited by immiscible gas bubbles, the effective density of the entrained fluid had to be increased. It was therefore treated as an adjustable parameter. The density of this arbitrary entrained fluid was set as 1000κ (kg/m^3) where κ is a dimensionless fitting parameter.

Figure 3 represents a generic nozzle with all its geometric parameters, using this generic design any nozzle can be constructed using the appropriate values of the geometric parameters. In this study 6 geometries were considered using the geometric values provided in Table 2. The selected geometries shown in Figure 4 vary in geometric parameters like mixing tube length, converging section geometries etc. All the geometries given in figure were modelled using axi-symmetric approximation and the gas inlet was modelled as a slit of equivalent area. Water was used as the motive fluid and air was replaced by an arbitrary miscible fluid with density $1000\ \kappa$ (kg/m^3). The ejector is oriented in down-flow fashion where water enters from the top liquid nozzle and exits from the bottom.

3.2 Computational model

Single phase turbulent flow of two miscible fluids of different densities was simulated using the Reynold's averaged Navier – Stokes equations. The turbulent flow was simulated using the Realizable k-ε model. The species equation was only solved for the secondary fluid [26]. All simulations were performed using the commercially available CFD software FLUENT 14.5. For the sake of brevity, the model equations are not described here and can be found in User guide [27]. Grid independence studies were performed using three grids 1x (~50000), 2x (~100000) and 4x (~200000) for each geometry. Simulations were performed using each grid and it was found that the maximum percent difference between 1x and 2x grid size was less than 5% and the maximum difference between 2x and 4x was less than 1%. As this error is much less than the error of experimental measurement 2x grid (~100000 computational cells) was selected for all the further studies. The details of the number of grids points and average area of cell for six different nozzle–diffuser geometries are given in Table 3.

As the volumetric flow rates of water through the nozzle are known, the inlet velocity was used as the boundary condition for primary liquid. The other opening of the suction chamber through which secondary fluid gets entrained, was the inlet with a value of 0 gauge pressure, as it is open to the atmosphere. The ejector outlet also was considered at 0 gauge pressure. The no-slip boundary condition was enforced at the walls of the ejector and the nozzle using standard wall function. The second order upwind discretization scheme was used for the momentum, mass fraction, turbulent kinetic energy and turbulent energy dissipation rate and SIMPLE scheme was used for the pressure–velocity coupling. A relaxation factor of 0.3 and 0.4 was used for the pressure and momentum respectively, while a factor of 0.4 was used for turbulent kinetic energy and turbulent energy dissipation rate. The solution was initialized by taking the ejector geometry completely filled with stagnant secondary fluid. The solution was iterated until convergence was achieved, such that the residue for each equation was well below 10^{-5}.

4. Results and discussion

The model was solved for the velocity, mass fraction of the secondary fluid and pressure across the ejector. The solution of these equation provide detailed results on velocity, turbulence characteristics and extent of secondary fluid inside the ejector. A sample of simulated velocity, pressure and mass fraction of the primary phase in the form of contour plots are shown in Figure 5. As seen from the velocity contour plot the falling primary jet creates a conical jet envelop in which primary and secondary fluids flow together causing the induction. However, the jet slowly diffuses and becomes a mixture as can be seen in the contours of mass fraction. This jet envelop does not depend upon the jet velocity and is a constant for all the flow rates i.e. when the flow rate is changed the actual values of velocity will change but not the shape of the jet envelope. The lowest pressure region in the whole ejector geometry is at the end of the mixing tube and the highest pressure region is in the liquid nozzle which is expected.

In the preliminary simulations two hypothesis were tested; first is correlation/similarity between induction of arbitrary fluid and experimentally observed gas induction. The second is whether induction of arbitrary secondary fluid can be fitted to experimental results using the adjustable density parameter κ. To test the first hypothesis simulations were performed using $\kappa = 1$ for ejector A, B and C. The results from the simulations are in the form of flow rates of primary and secondary fluids. The results were normalized to compare the trends from the simulated data and the experimental data presented by Bhutada et al [6]. In the normalization process the simulated and experimental values were divided by or taken ratio with a single

liquid flow rate and the corresponding gas induction reading. In this way all the data sets for different ejectors have one common point and rest of the data set is the ratio with respect to the selected data point. The selected data point for this exercise is 1.067 kg/s and the corresponding fluid induction value for each set of data. Normalized simulated results were plotted with the normalized experimental data as seen in Figure 6. It can be seen that the normalized gas induction trends were successfully captured using the single phase model indicating that induction trends of arbitrary fluid and gas are similar and depend upon the geometry of the ejector.

Even as similar trends between volumetric liquid and gas induction were observed the actual values were very different. Therefore the value of the density parameter, κ of the secondary fluid was reduced. The logic behind this is as the gas induction depends upon kinetic energy imparted by the down-flowing jet, any decrease in the density of the surrounding fluid will result in the increase in overall volumetric fluid induction as shown in Figure 7. As the density of the secondary fluid decreases the volumetric induction rate increases. Thus the density parameter, κ, may be used as an adjustable parameter to fit the simulated induction rate of arbitrary fluid with the experimentally observed gas induction rate. Figure 7 also indicates that $\kappa = 0.4$ is the best match for experimental data for ejector B.

Experimental pressure drop was compared to the simulated pressure drop for the geometries B and OG and at parameter $\kappa = 1, 0.4$. As seen in Figure 8 the simulation results are in line with experimental observation that the ejector pressure drop is insignificant as compared to the nozzle pressure drop. Even when the induction at different κ values is different there is no realistic impact on the overall pressure drop of the whole system. This reinforces the basic assumptions that the driving force for gas induction is power imparted by the liquid nozzle. The resultant flow and pressure in the ejector is linked to the geometry of the ejector and depends upon the geometry of the ejector, power of the nozzle and the properties of the fluid.

Similar to Ejector B; fitting exercises were performed for different ejector geometries to correlate the secondary fluid induction with the experimental values using a mathematical parameter. The ejector geometries considered in this exercise are different in specific geometric parameters like mixing tube length, nozzle diameter or diffuser geometry etc. Furthermore, an attempt was made to club different geometries into specific groups making the parametric study easier. For example ejector C, C1 and C2 have identical geometries with the only exception of the mixing tube length. Here, the goal is to analyse each aspect of the ejector geometry and

to coherently correlate any geometric parameter to a mathematical parameter like κ. While experimental and pure correlative studies can make system specific prediction there is a need for a model that may predict the impact of a geometric parameter on a more general way.

The parameters like suction chamber geometry, distance between nozzle and mixing tube, mixing tube length, nozzle diameter and diffuser section were studied computationally. The experimental data was used wherever available. As seen in Figure 9a different configurations suction chamber geometries were made ranging from completely uncovered suction chamber to partially covered and finally to a standard suction chamber geometry as shown in different ejectors in Figure 4. Rest of the geometric parameters were kept constant including mixing tube length and diffuser length and divergence angle. Simulations were performed using the CFD model described in section 3 and keeping the secondary fluid density as 1000 kg/m^3 (κ = 1). Figure 9b shows the simulation results for the gas induction simulations using different suction chamber assembly. There is virtually no change in the gas induction for different geometries as all values lie within 5 % tolerance of each other. Hence, there is no significant impact of the suction chamber geometry on gas induction. Similar results were presented by Yadav et al [25] that the gas induction is independent of suction chamber geometry as long as $D_S / D_N > 4$ which in each of the considered experimental and simulations case is true. Hence, for the range of parameters considered in the present work, suction chamber geometry has no impact on gas induction.

Influence of the distance between nozzle outlet and the mixing tube inlet on the gas induction was investigated. A new parameter called the projection ratio was defined as $\left(L_{NM} / D_{MT} \right)$. Simulations were performed keeping the κ = 1. Projection ratio parameter was varied from 1.5 to 6.5. The results show that the gas induction is not affected by the PR beyond the value 4.5 as shown in Figure 10. Similar observations were made by Bhutada et al [4] (PR > 4) and Yadav et al [25] (PR > 5) experimentally and in numerical studies respectively. This is indicative of the fact that after a certain length the momentum transfer between the primary and the secondary fluid slows down and the jet flows as a mixture of the two fluids.

There is extensive data by Bhutada et al [5] on the effect of the length of mixing tube on gas induction in the ejector. From the published data, three geometries were selected having the

ratio of mixing tube length and diameter of mixing tube $\left(L_{MT} / D_{MT} \right)$ of 0, 4 and 8. These geometries C, C1 and C2 are similar in every respect except for the mixing tube geometry. Simulations were performed on all the three geometries and an attempt was made to fit volumetric gas induction by varying the parameter κ. These results are shown in Figure 11, the values of κ decrease as the mixing tube length increases. Hence, a direct correlation between the fitting parameter and mixing tube length may be established.

Gas induction also depends upon the ratio of two individual geometric parameters of nozzle diameter and mixing tube diameter. As, the impact of one is always in tandem with the other, the ratio of these two diameters is studied as a single parameter. Data is available for three different ratios of nozzle diameter and mixing tube diameter namely, $D_N / D_{MT} = 5/16, 8/16, 10/16$. The impact of this parameter was studied with respect to the entire geometry, since it was established that the liquid nozzle and ejector configuration forms a decoupled system the impact of liquid nozzle diameter can be established independent of ejector geometry. Three different geometries, Ejector A, B and C were simulated with three nozzle 5, 8 and 10 mm. By adjusting the value of parameter κ the simulated induction rate was fitted to the experimental values published by Bhutada et al [6]. Figure12 shows the comparison of experimental results compared with the simulated results for three different ejector configurations and three different D_N / D_{MT}.

All the geometries selected in this study have a diffuser angle of 5 °. Hence, numerical studies were performed to study the impact of the diffuser angle of the ejector. Changes were made in geometry Ejector C2 and 6 different geometries were made with the 0, 2.5, 5, 7.5, 10 and 90° diffuser angle. Simulations were performed at κ = 0.325 and the results for 1 kg/s primary liquid flow rate are shown in Figure 13. The maximum induction was achieved at 5° diffuser angle. Similar conclusions were made by Bhutada et al where 5° was considered the optimum angle for diffuser geometry. The function of the diffuser geometry is to recover pressure before the fluid mixture leaves the ejector. If the recovery is slow like in the case of straight pipe diffuser and 2.5° diffuser angle the losses related to friction are greater. If the recovery is very quick like in the case of angles 7.5° and 10° there is a very early separation of the jet from the wall leading to high form drag and high backflow from the circumferential area of the outlet

of the ejector. If there is no diffuser section (90° diffuser angle) and the fluid exits the ejector just after the point of maximum velocity and maximum pressure (0 gauge pressure), this would significantly decrease the volumetric induction.

Table 4 shows the different values of geometric parameters and the corresponding value of κ used to fit the gas induction values at those conditions. From the published works and simulations with different ejector geometry it is clear that gas suction chamber geometry has no impact on gas induction and if $L_{NM}/D_{MT} > 4.5$ the impact of this parameter can be neglected. Hence, in this discussion these two parameters are not considered. While, the diffuser angle does impact the gas induction the reported literature and numerical studies points to the conclusion that at 5 ° diffuser angle the gas induction is maximum. Hence, all further studies will be done at the same diffuser angle. The parameters that were considered are mixing tube length and ratio of diameters of nozzle and mixing tube.

Figure 14b shows the variation of fitting parameter with the ratio of mixing tube length and mixing tube diameter $\left(L_{MT}/D_{MT}\right)$, the relationship as seen in the figure is straightforward as the mixing tube length increases the value of the fitting parameter goes down as shown in Equation 1.

$$\kappa = aL_{MT}^{b} \tag{1}$$

Where b = -0.009 and a = 1 (8 mm nozzle); 1.2 (10 mm nozzle); 5.5 (5 mm nozzle)

Interesting results were seen in the study of D_N/D_{MT} parameter as shown is Figure 14a, the ratio of fitting parameter is basically same for ejector A, B and C while the actual values are different. Hence, it can be concluded that the impact of the liquid nozzle on a system is same for all three cases and is a constant for a given system. As not enough data is available to develop a correlation for D_N/D_{MT} as we have only three data points. However, the values for the 3 cases can be used straightaway for further simulations.

The Equation 1 was used to predict the gas induction in the geometry Ejector OG. The results of this prediction are shown in Figure 15 along with the measured values of gas induction in

ejector OG. As seen in the figure the simulated values are in reasonable agreement with the experimental values. The parameter κ may be interpreted as a quantity representing interphase drag. The developed approach and the model may therefore be used to estimate the gas induction values in a new geometry within the error limit of the measurement.

5. Conclusions

Experimental results in tandem with flow modelling was employed in order to develop an approach for estimating the gas induction in gas liquid ejector. A simplified single phase fluid CFD model was used to estimate gas induction using a fitting parameter κ which was shown to have significant relationship with various geometric parameters of the gas-liquid ejector. Each of the parameters were individually analysed using computational or experimental studies in order to derive a coherent and usable correlation to predict gas induction in an ejector. Furthermore, geometric parameters of ejector were analysed in order to develop a better understanding of significance and sensitivity of the various parameters specific conclusions are listed below:

1. Induction of any fluid either gas or liquid in a specific ejector geometry follow similar trends and show a strong dependence on the geometric parameters of the ejector.
2. It was shown that the dependence of gas induction was not sensitive to suction chamber geometry (< 5%).
3. The relationship of gas induction with projection ration is insignificant for PR > 5.
4. It was shown that maximum gas induction occurs when the diffuser angle is 5°.
5. Gas induction may be fitted to experimental gas-liquid gas induction values using a fitting parameter, this fitting parameters depends on geometric parameters like $\left(L_{MT}/D_{MT}\right)$ and D_N/D_{MT}.

Acknowledgement

Deepankar V Sharma acknowledges Council for Scientific and Industrial Research (CSIR) for Senior Research Fellowship. Authors acknowledge the funding from CSIR's Indus MAGIC program [CSC123].

Symbols and Notations

Sr. #	Symbol	Quantity	Unit
1	u	Velocity	m/s
2	ρ	Density	kg/m^3
3	$\vec{g}$	Directional Gravity	m/s^2
4	D	Diameter	m
5	μ	Viscosity	$Pa.s$
6	ε_G	Gas Hold-up	-
7	σ	Surface Tension	N/m
8	ΔP	Pressure drop	Pa
9	$U_{G,Sup}$	Superficial gas velocity	m/s
10	M	Mass Entrainment	kg/s
11	L	Length	m
12	A	Area ratio	m^2
13	κ	Fitting parameter	-

Subscript/Superscript

Sr #	Subscript/Superscript	Quantity
1	e	Entrained Fluid
2	m	Motive Fluid
3	G/L	Gas/Liquid
4	MT	Mixing Tube
5	N	Nozzle
6	NM	Distance b/w nozzle and mixing tube
7	S	Suction chamber
8	r	Ratio

References

1. Zahradnik, J.; Fialova, M.; Linek, V., Subjuke, J., Reznickova, J. Dispersion efficiency of ejector type gas distributors in different operating model. *Chem. Eng. Sci.* **1997**, 52, 4499.
2. Bin, A.K. Gas entrainment by plunging liquid jets. *Chem. Eng. Sci.***1993**, 48, 3585.
3. Bhutada, S. R.; Pangarkar, V. G. Gas induction and hold-up characteristics of liquid jet loop reactors. *Chem. Eng. Comm*. **1987**, 61, 239.
4. Fadavi, A.; Chisti, Y. Gas-liquid mass transfer in novel forced circulation loop reactor. *Chem. Eng. J.* 2005, **112**, 73.
5. Havelka, P.; Linek, V.; Sinkule, J.; Zaheadnik, J.; Fialova, M. Effect of the ejector configuration on the gas suction rate and gas hold up in the ejector loop reactors. *Chem. Eng. Sci.***1997**, 52, 1701.
6. Evans, G.M.; Bin, A.K.; Machniewski, P.M. Performance of confined plunging liquid jet bubble column as a gas-liquid reactor. *Chem. Eng. Sci.* **2001**, 56, 1151.
7. Sotiriadis, A.A.; Thorpe, R.B.; Smith, J.M. Bubble size and mass transfer characteristics of sparged downwards two-phase flow. *Chem. Eng. Sci.***2005**, 60, 5917.
8. Tinge, J.T.; Rodriguez Casado, A.J. Influence of pressure on the gas hold-up of aqueous activated carbon slurries in a down flow jet loop reactor. *Chem. Eng. Sci.***2002**, 57, 3575.
9. Havelka, P.; Linek, V.; Sinkule, J.; Zaheadnik, J.; Fialova, M. Hydrodynamic and mass transfer characteristics of ejector loop reactors. *Chem. Eng. Sci.***2000**, 55, 535.
10. Davies, G.S.; Mitra, A.K.; Roy, A.N. Momentum transfer studies in ejectors. *Ind. Eng. Chem. Process Design Dev*. **1967**, 6, 293.
11. Acharjee, D.K.; Bhat, P.A.; Mitra, A.K.; Roy, A.N. Studies on momentum transfer in vertical liquid jet ejectors. *Indian J. Tech*. **1975**, 13, 205.
12. Bhutada, S. R.; Pangarkar, V. G. Solid suspension and mixing characteristics of liquid jet loop reactors. *Chem. Eng. Sci*. **1989**, 44, 2384.
13. Dutta, N.N.; Raghavan, K.V. Mass transfer and hydrodynamic characteristics of loop reactors with down flow liquid jet ejector. *Chem. Eng. J*. **1997**, 36, 111.

14. Bhutada, S.R. Design f liquid jet loop reactors, Ph. D. (Tech) Thesis, University of Mumbai, 1989.
15. Ben Brahim, A.; Prevost, M. &Bugarel, R. Momentum transfer in a vertical down flow liquid jet ejector: Case of self-gas aspiration and emulsion flow. *J. Multiphase Flow*. **1984**, 10, 79.
16. Bhat, P.A.; Mitra, A.K.; Roy, A.N. Momentum transfer in a horizontal jet liquid jet ejector. *Can. J. Chem. Eng.***1972**, 50, 313.
17. Cramers, P.H.M.R.; Beenackers, A.A.C.M. Influence of ejector configuration, scale and the gas density on the mass transfer characteristics of gas-liquid ejectors. *Chem. Eng. J.***2001**, 82, 131.
18. Dirix, C.A.M.C. & van der Wiele, K. Mass transfer in jet loop reactors. *Chem. Eng. Sci.***1990**, 42, 2333.
19. Lehtonen, J.; Kaplin, J.; Salmi, T.; Haario, H.; Vuori, A.; Tirronen, E. Modelling and scale-up of a loop reactor for hydrogenation processes. *Chem. Eng. Sci.***1999**, 51, 2793.
20. Salmi, T.; Lehtonen, J., Kaplin, J., Vuori, A., Tirronen, E., Haario, H. A homogeneous-hetrogeneously catalysed reaction system in a loop reactor. *Cat. Today.***1999**, 448, 139.
21. Kim, M.I.; Kim, O.S.; Lee, D.H.; Kim, S.D. Numerical and Experimental investigations of gas-liquid dispersion in an ejector. *Chem. Eng. Sci.* **2007**, 62, 7133.
22. Utomo, T.; Jin, Z.; Rahman, Msq.; Jeong, H.; Chung, H. Investigation on hydrodynamics and mass transfer characteristics of a gas-liquid ejector using three dimensional CFD modelling. *J. Mech. Sci. Tech.***2008**, 22, 1821.
23. Yadav, R.L.; Patwardhan, A.W. Design aspects of ejectors: Effect of suction chamber geometry. *Chem. Eng. Sci.* **2008**, 63, 3886.
24. Kandakure, M.T.; Gaikar, V.G.; Patwardhan, A.W. Hydrodynamic aspects of ejectors. *Chem. Eng. Sci.* **2005**, 60, 6391.
25. Kim, O.G.; Lee, Y.; Lee, D.H. Hydrodynamic characteristics of a horizontal flow ejector in a rectangular chamber. *Korean J. Chem. Eng.***2009**, 26, 288.
26. Ranade, V.V. *Computational Flow Modeling for Chemical Reactor Engineering,* 1st Edition; Academic Press: California, 2002; pp 41.
27. ANSYS® Fluent, Release 14.5, Fluent Theory Guide, Basic Fluid Flow (1), Turbulence (4), Species Transport and Finite Rate Chemistry (7), ANSYS, Inc.

List of Figures

Figure 15: Validation of single phase model: Gas Induction in Ejector OG at 8 and 10 mm successfully predicted

List of Tables

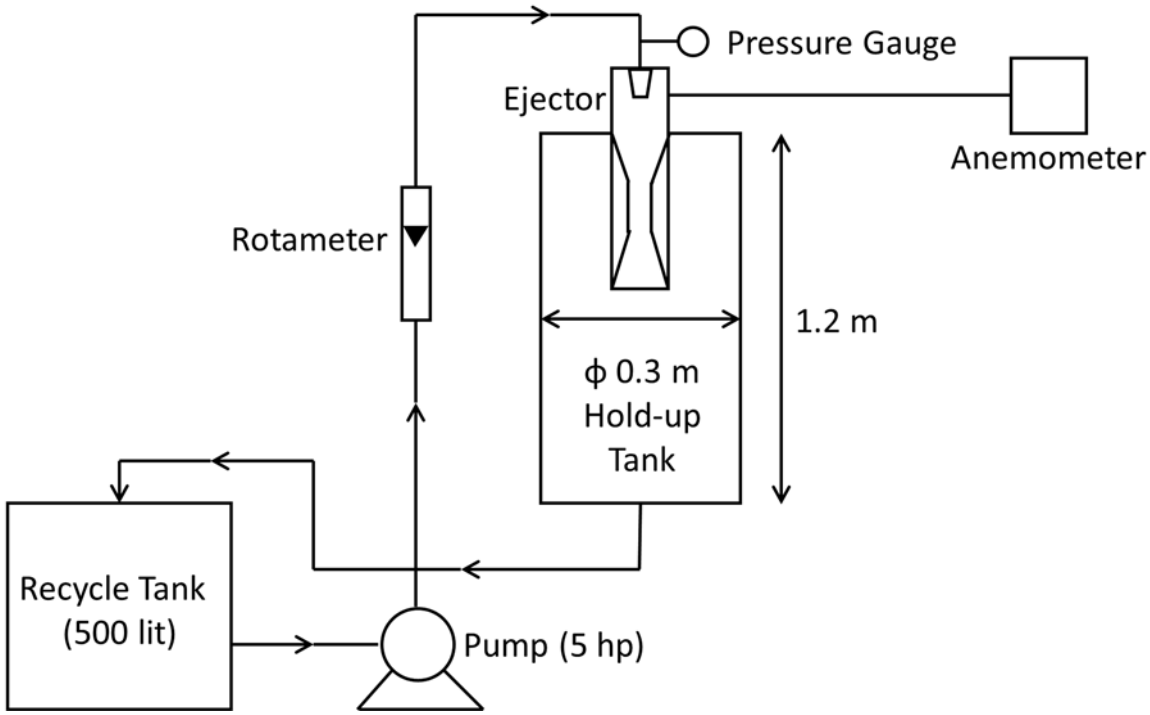

(a)

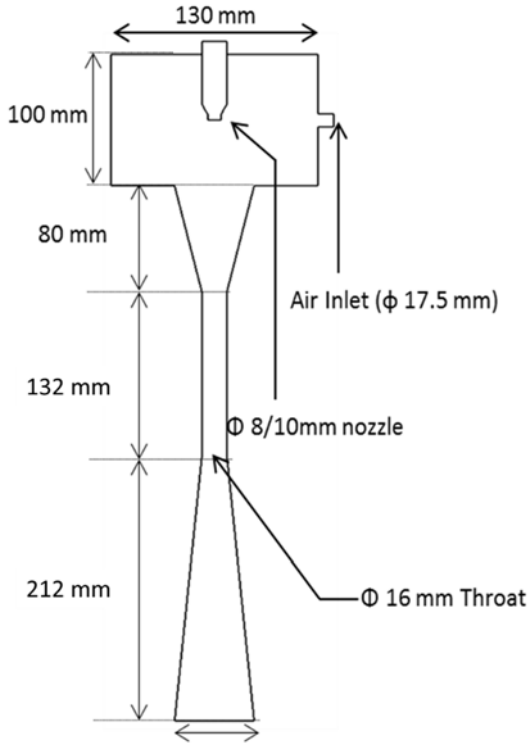

(b)

Figure 1: Description of Experimental set up (a) Schematics for the set up (b) Detailed drawing of Jet Ejector

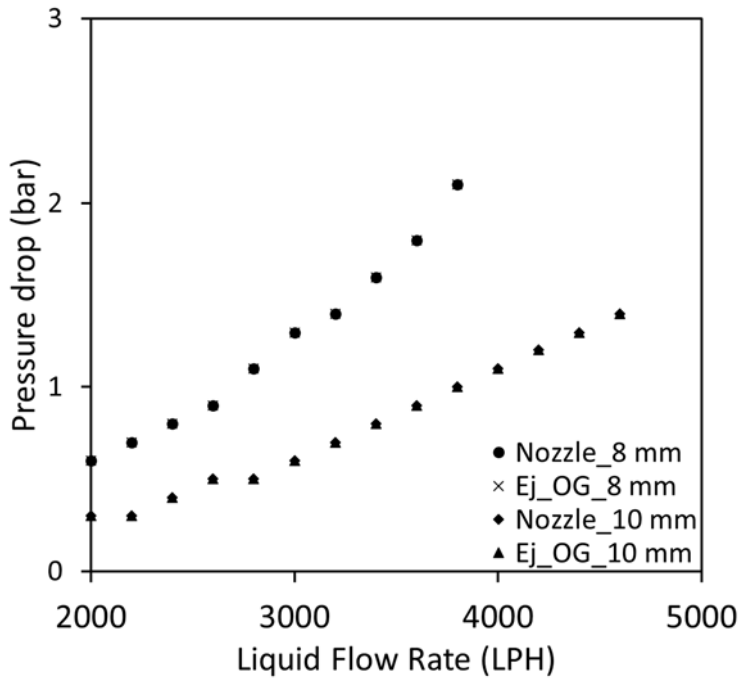

(a)

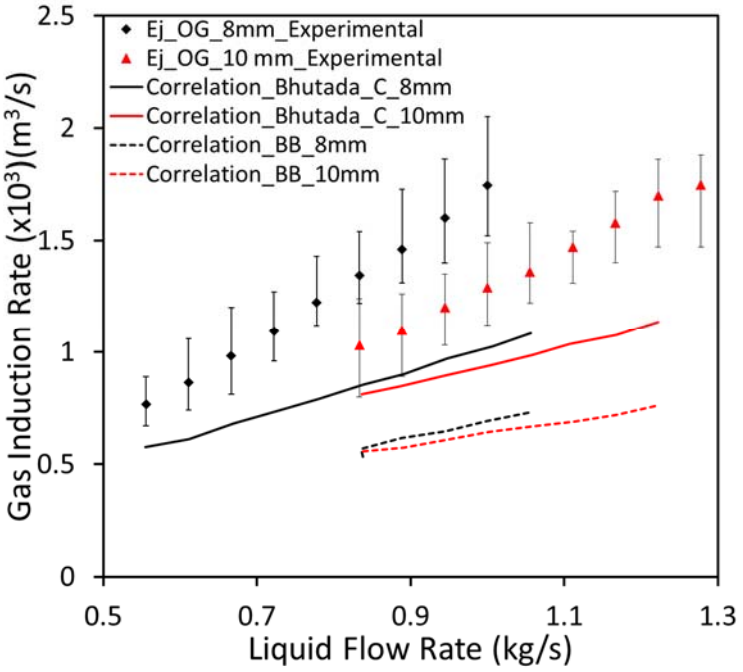

(b)

Figure 2: Experimental Results (a) Comparison of Pressure drop with and without Venturi Geometry, (b) Measured Gas Induction rates compared to predicted values using correlations by Bhutada et al & Ben Brahim et al

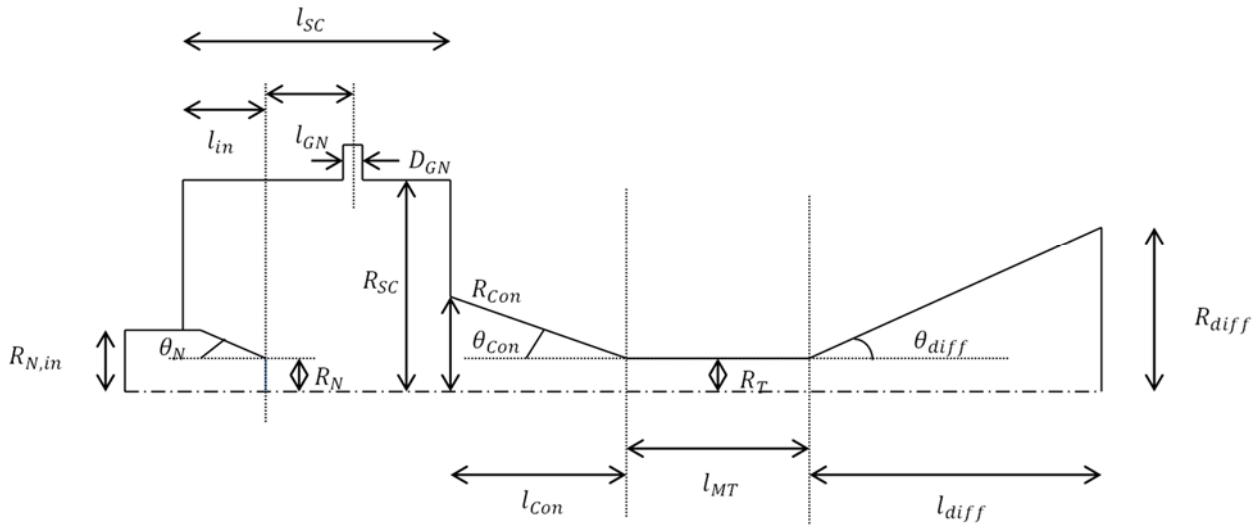

Figure 3: A Schematic of a generic nozzle

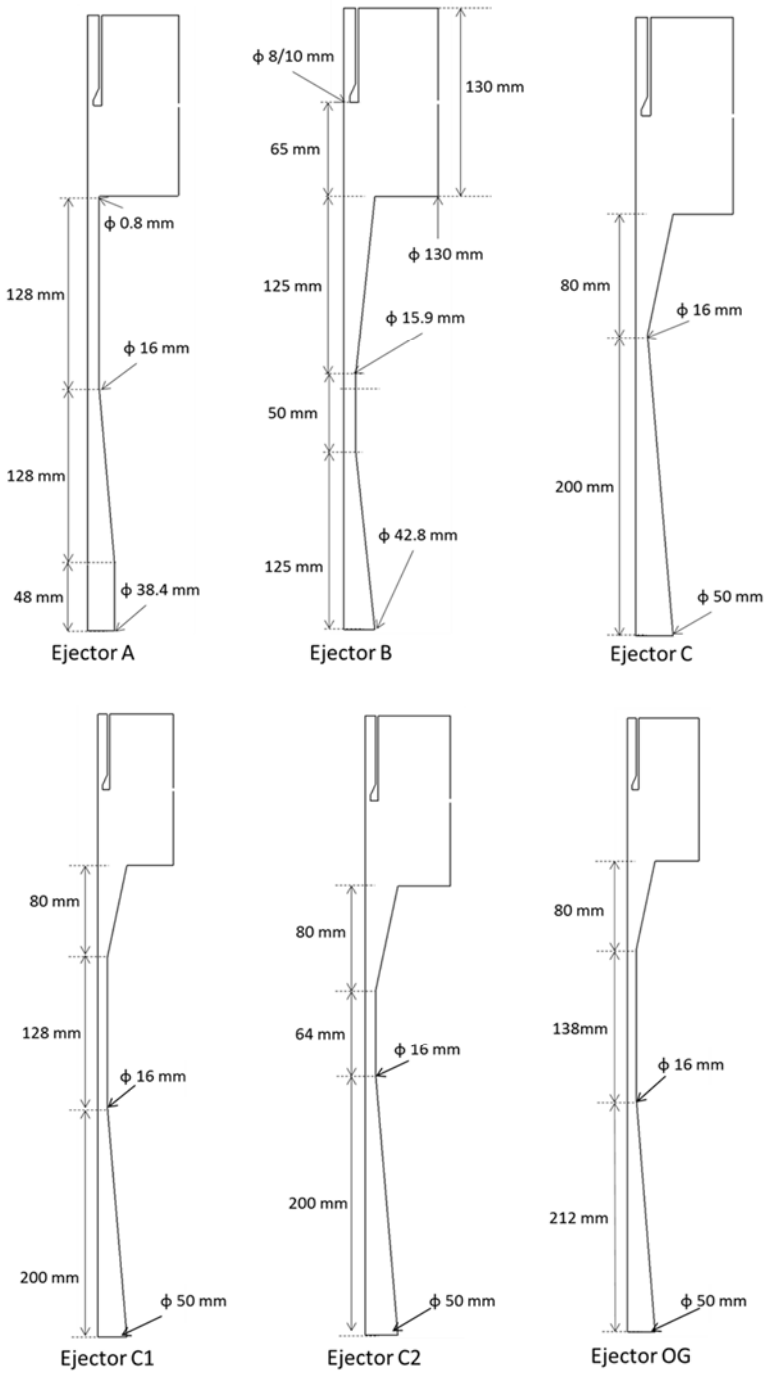

Figure 4: Selected geometries with varying geometric parameters

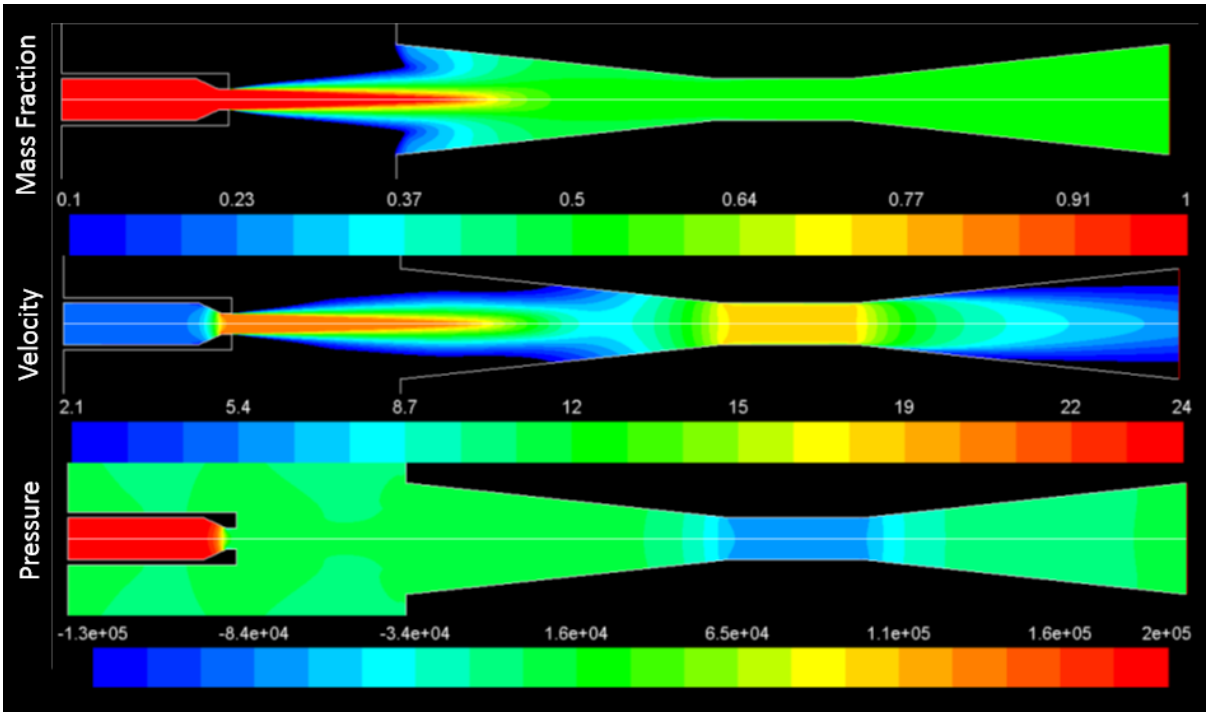

Figure 5: Contour Plots for Velocity (m/s), Mass fraction and Pressure (Pa) in Ejector B at 1.25 kg/s Primary fluid inlet and $\kappa = 1$

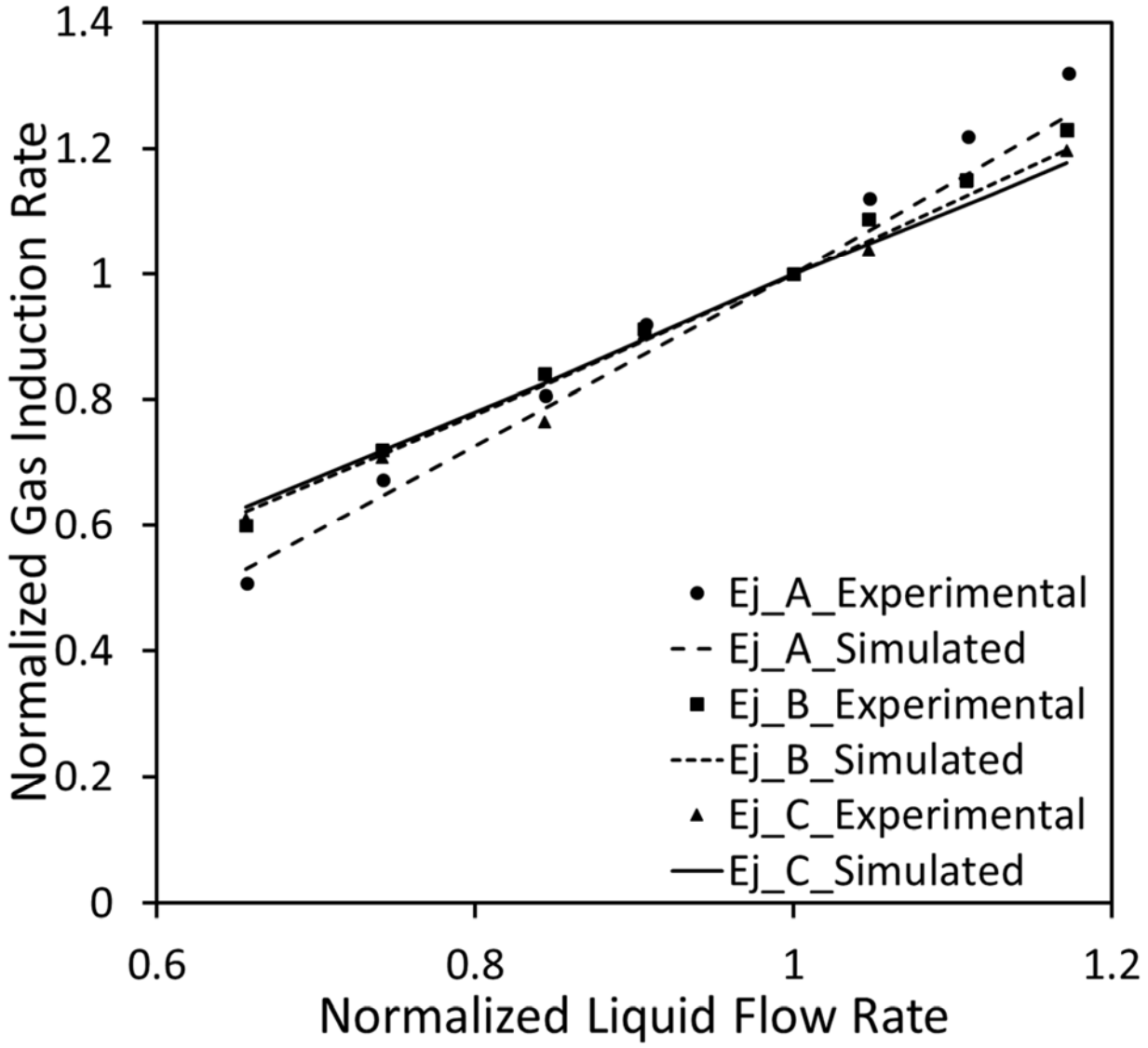

Figure 6: Normalized Experimental Gas Induction Rates (Bhutada et al) compared to Normalized Simulated Gas Induction Rates ($\kappa = 1$) for Ejector A, B and C; 8 mm nozzle

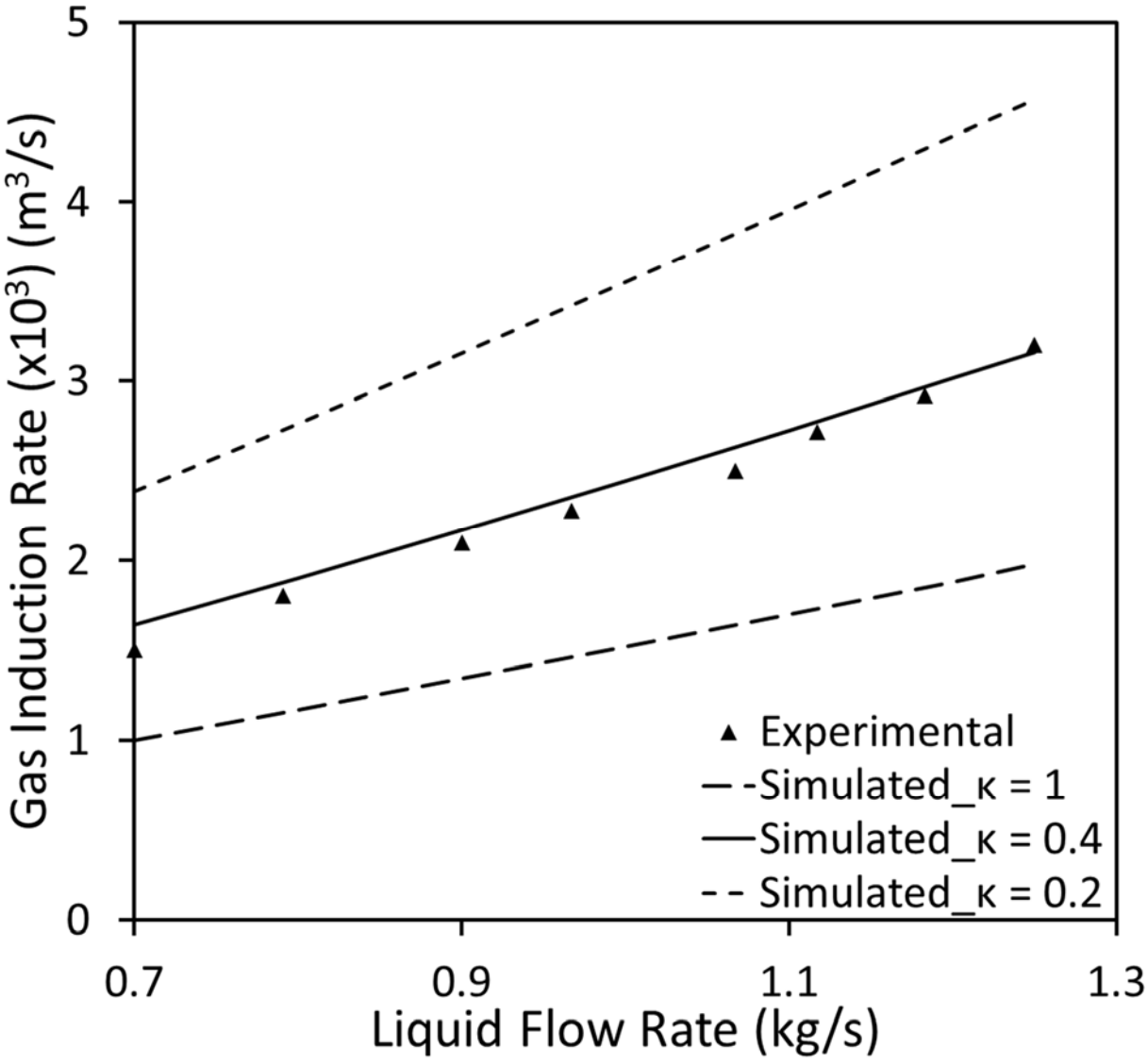

Figure 7: Fitting of Simulated Gas Induction rate by varying κ for Ejector B; 8mm nozzle

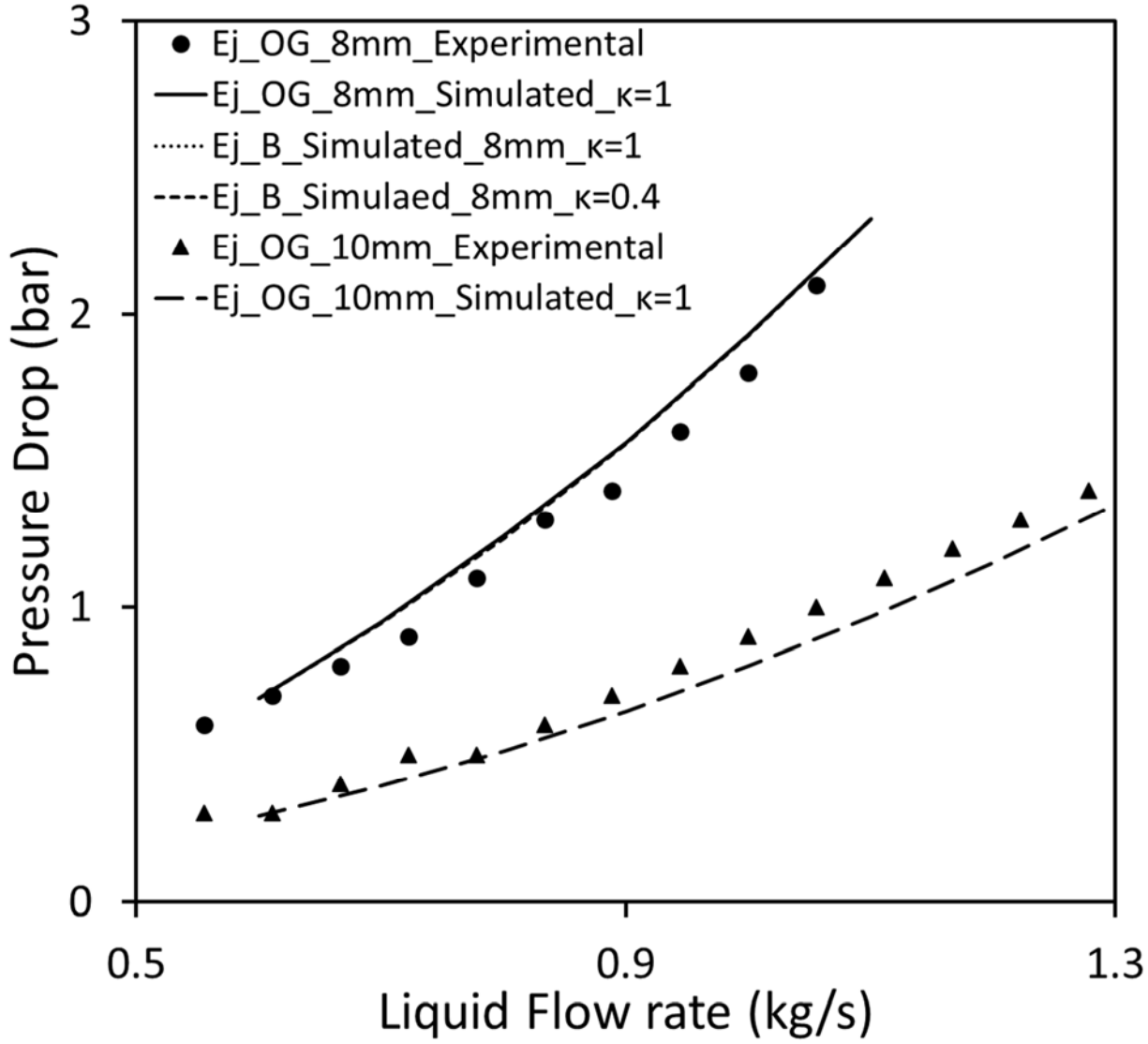

Figure 8: Experimental Pressure Drop against Simulated Pressure drop for Ejector OG and B; 8 & 10 mm nozzle and κ = 1, 0.4

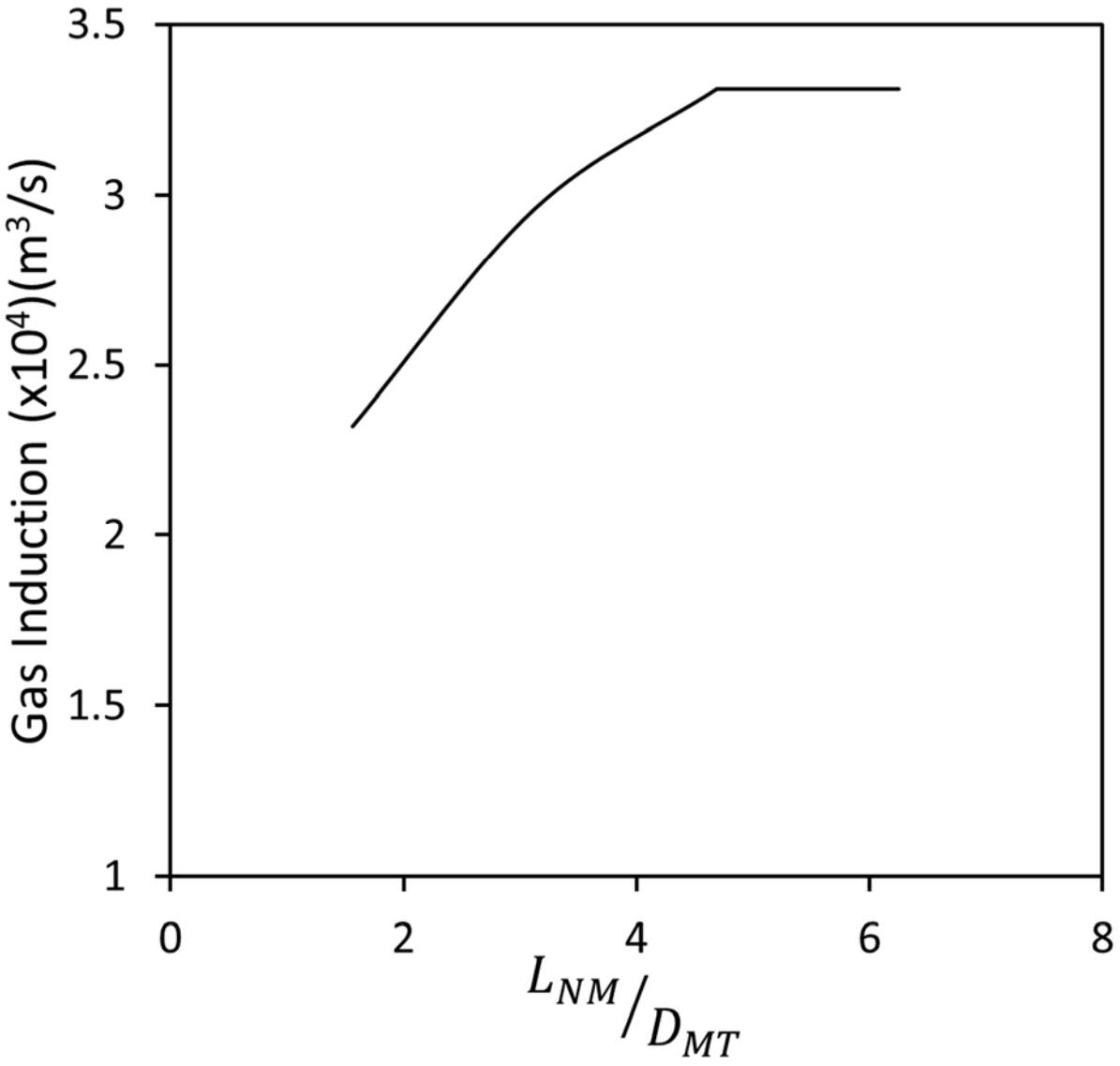

Figure 9: Effect of distance between Nozzle and Mixing tube L_{NM}/D_{MT} at 1.25 kg/s Liquid flow rate and κ = 1

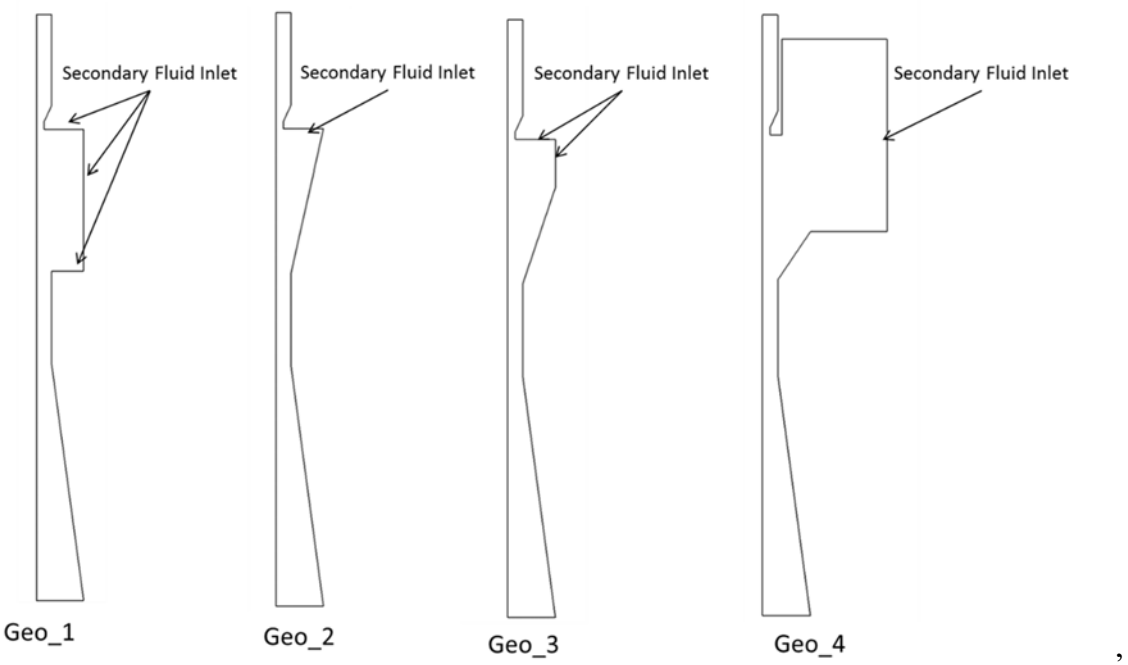

(a)

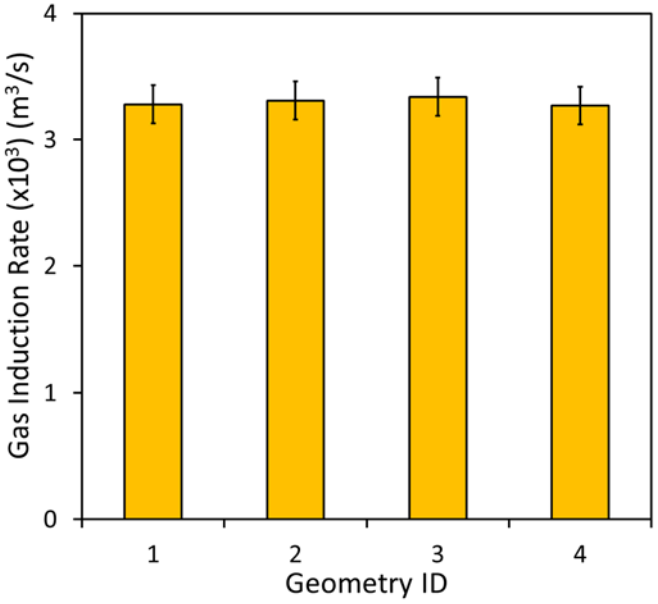

(b)

Figure 10: Effect of Suction Chamber Geometry (a) 4 Geometries with different suction chamber configurations (b) Simulation Gas Induction at 1.25 (kg/s) Liquid flow rate and κ =1

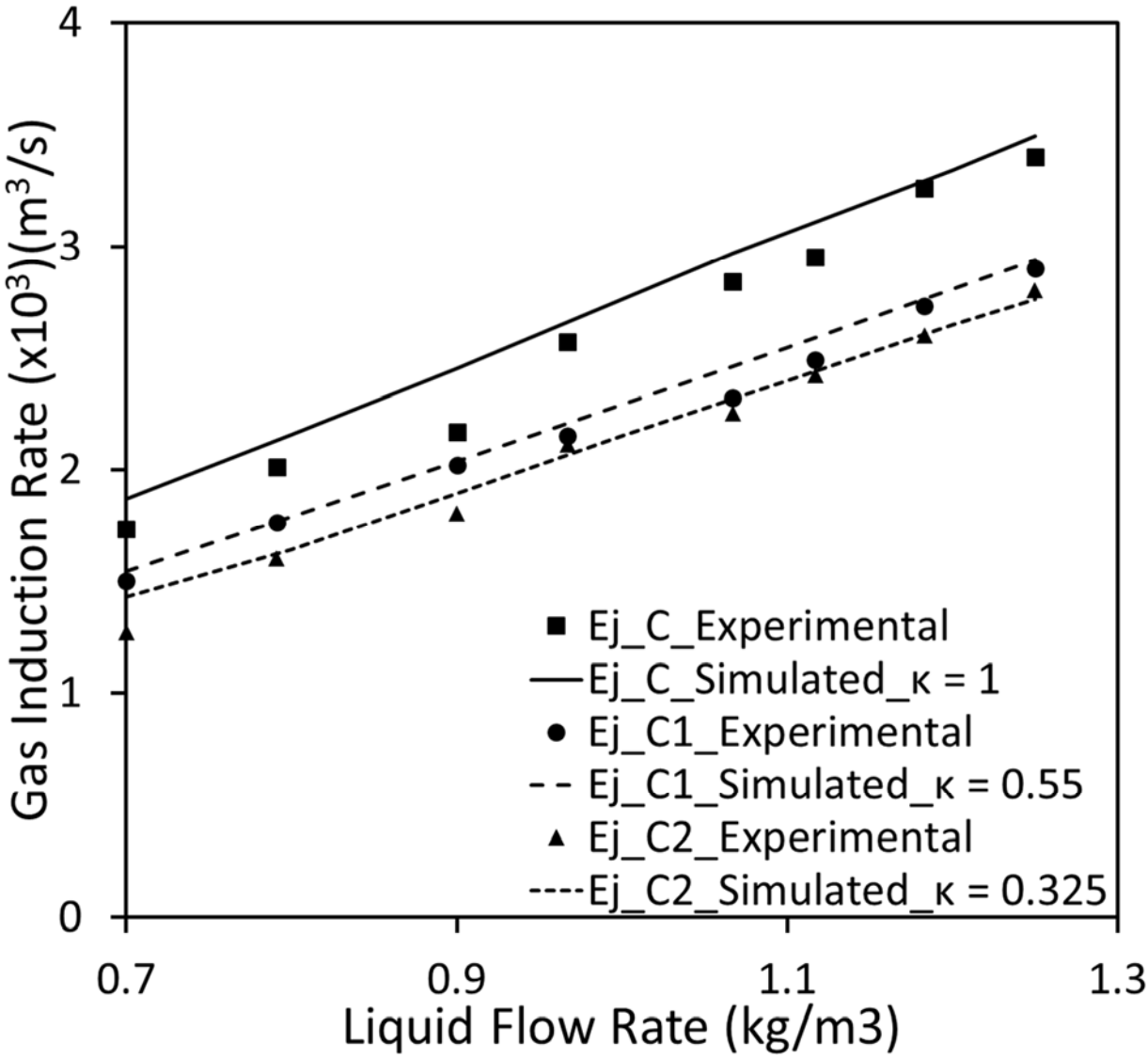

Figure 11: Fitting of Experimental Gas Induction using single phase model by varying κ for Ejector C $\left(L_{MT}/D_{MT} = 0\right)$, C1 $\left(L_{MT}/D_{MT} = 4\right)$ and C2 $\left(L_{MT}/D_{MT} = 8\right)$; 8 mm nozzle

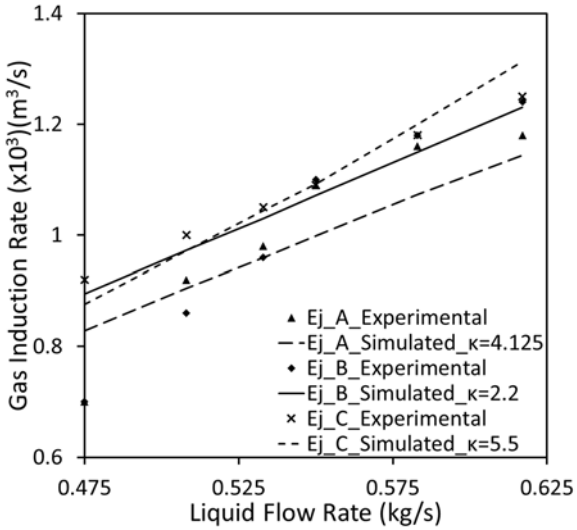

(a)

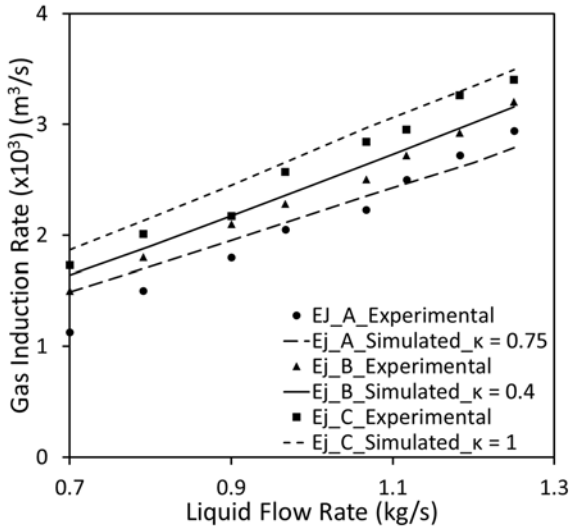

(b)

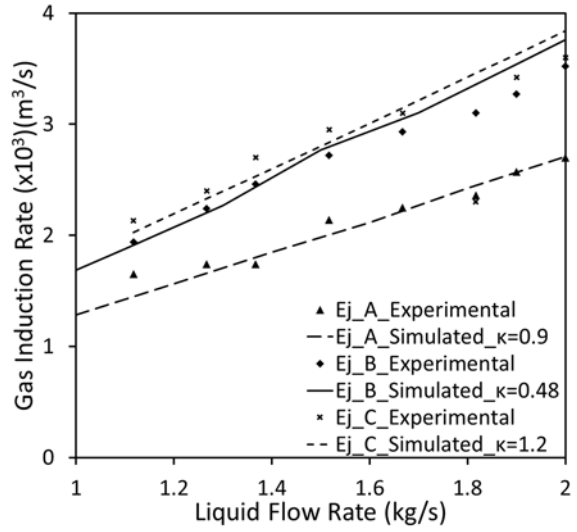

(c)

Figure 12: Fitting of experimental gas induction using single phase model by varying κ for Ejectors A, B and C and for (a) $D_N/D_{MT} = 5/16$; (b) $D_N/D_{MT} = 8/16$; (c) $D_N/D_{MT} = 10/16$

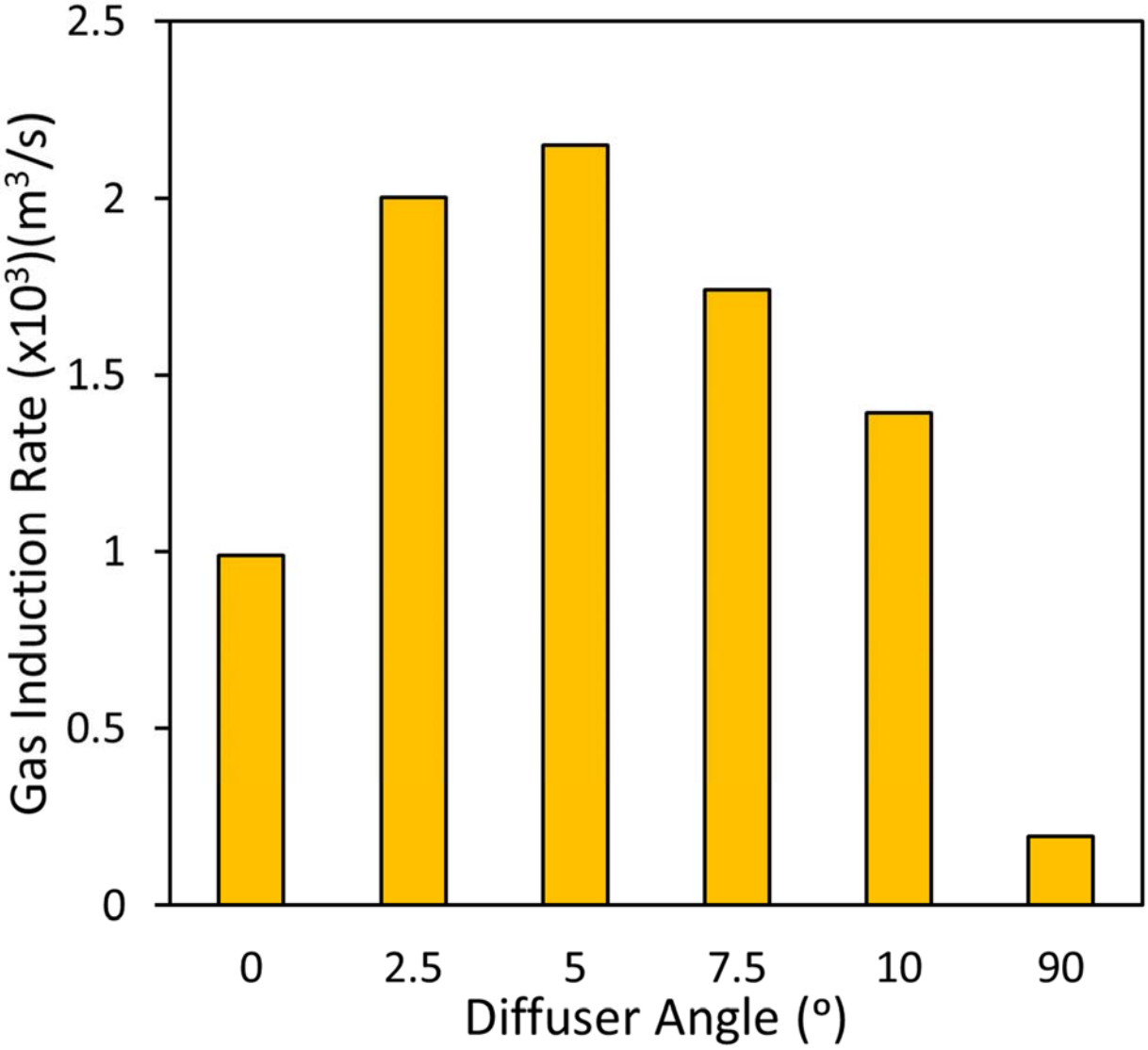

Figure 13: Gas induction at different diffuser angles ranging from 0° (Straight Pipe) to 90° (No diffuser) at for Ejector C2; 8 mm nozzle and $\kappa = 0.325$

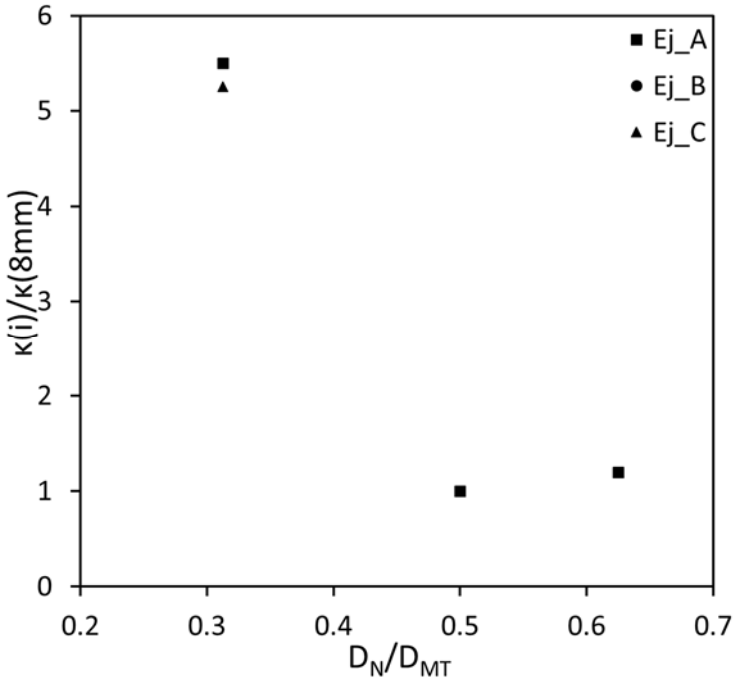

(a)

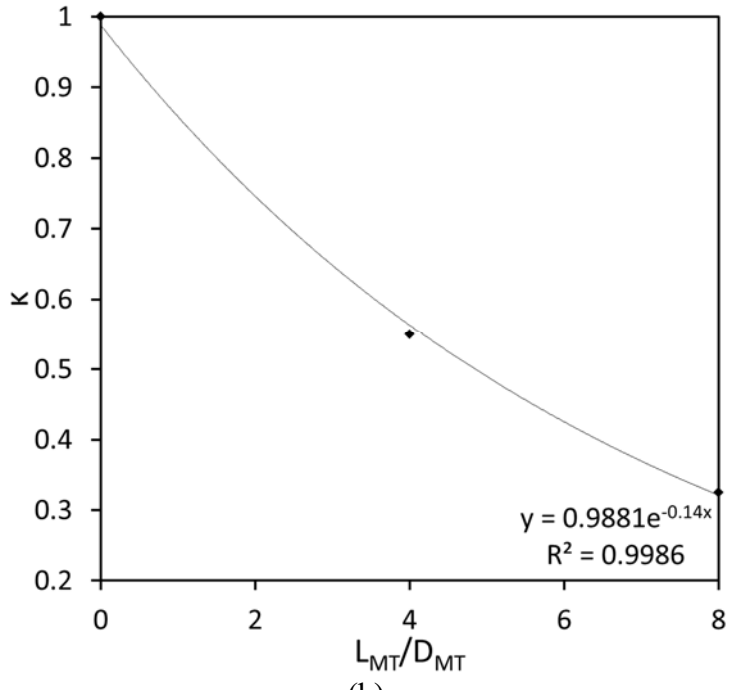

(b)

Figure 14: Variation of κ with different geometric parameters (a) Variation with D_N/D_{MT} (b) Variation with L_{MT}/D_{MT}

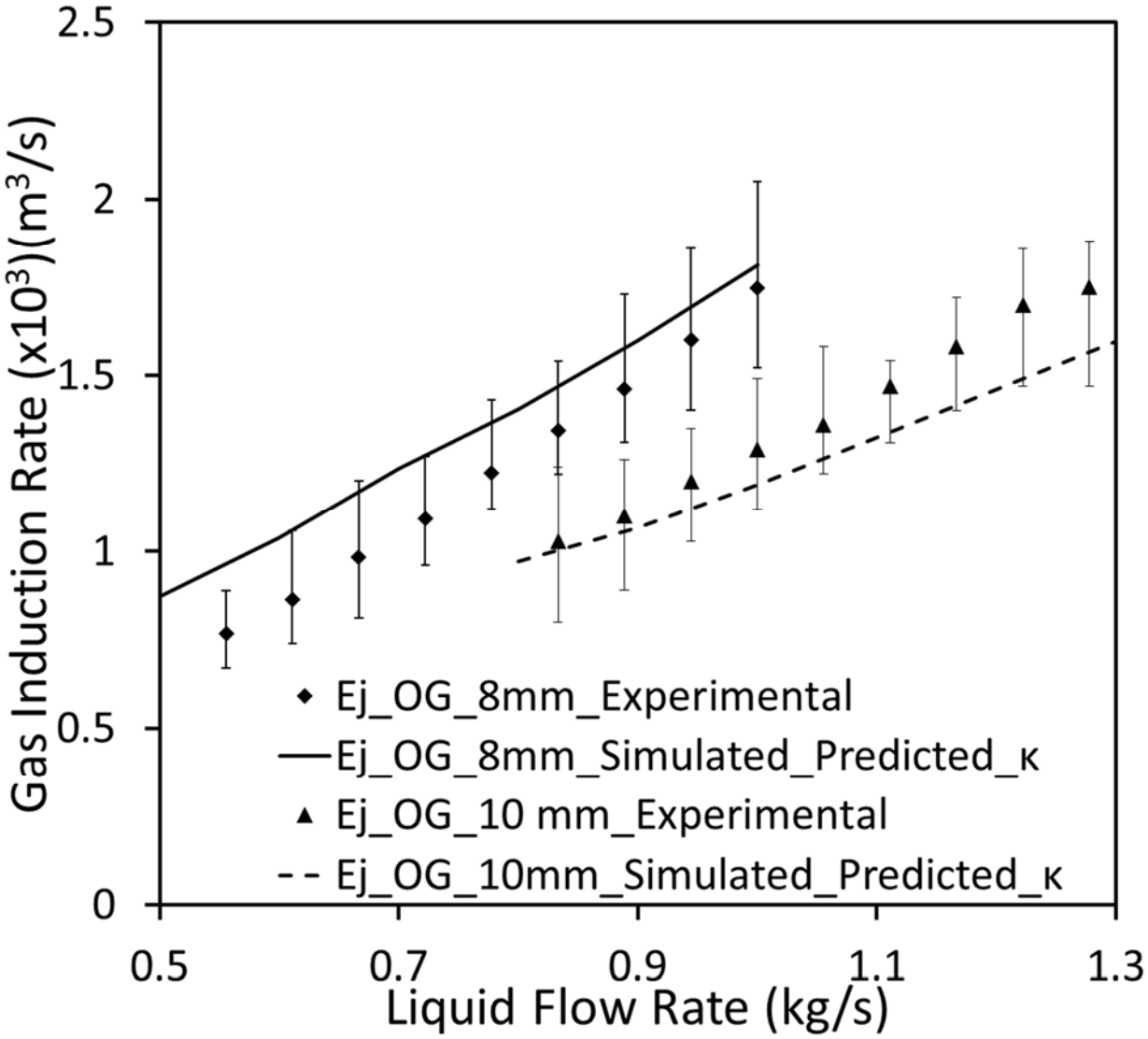

Figure 15: Validation of single phase model: Gas Induction in Ejector OG at 8 and 10 mm successfully predicted

Table 21 Correlations for gas induction reported in literature

Reference	Nozzle Diameter (mm)	D_N/D_{MT}	L_{MT}/D_{MT}	Diffuser Length & Angle (mm, °)	Correlation
Davis et al (1967)	0.808-2.676	4.5-15.72	9	30, 9.45	$Mr = k\left(\frac{\mu_m}{D_N \rho_m U_m}\right)^{-0.76} Ar^{0.4}\left(\frac{g\mu_m^4}{\rho\sigma_m^3}\right)^{-0.04}\left(\frac{\rho_m - \rho_{mix}}{\rho_m}\right)^{0.63}$
Bhat et al (1972)	1.9-4.49	2.06-4.87	5	50, 7.8	$Mr = 8.5\times10^{-2}\left(\frac{\Delta P_e}{\rho_e u_e^2}\right)^{-0.3} Ar^{0.46}\left(\frac{g\mu_m^4}{\rho\sigma_m^3}\right)^{-0.02}$
Acharjee et al (1975)	1.78-5.5	2.31-7.13	5	50, 7.8	$Mr = 5.2\times10^{-4}\left(\frac{\Delta P_e}{\rho_e u_e^2}\right)^{-0.305} Ar^{0.68}\left(\frac{g\mu_m^4}{\rho\sigma_m^3}\right)^{-0.305}$
Ben Brahim et al (1984)	2.5	2	7	92, 5	$Mr = 4.386\times10^{-3}\left(\frac{\Delta P_e}{\rho_e u_e^2}\right)^{-0.38}\left(\frac{g\mu_m^4}{\rho\sigma_m^3}\right)^{-0.01}$
Dutta and Raghwan et al (1987)	4.5, 6.5	2.77-4	2.77	80, 7.5	$Mr = 2.4\times10^{-3}\left(\frac{\Delta P_e}{\rho_e u_e^2}\right)^{-0.82}\left(\frac{g\mu_m^4}{\rho_m\sigma_m^3}\right)^{-0.01}$
Bhutada et al (1987)	5, 8, 10	1.6-3.2	0-8	200, 5	$Mr = C\left(\frac{\Delta P_e}{\rho_e u_e^2}\right)^A Ar^B$ $C = 5.58\times10^{-4}\,to\,9.67\times10^{-4}$ $A = -0.135\,to\,-0.202;\ B = 0.07\,to\,0.224$

Table 2: Values of geometric parameters for constructing various ejectors from the generic nozzle

Parameter (cm)	Ejector A	Ejector B	Ejector C	Ejector C1	Ejector C2	Ejector OG
$R_{N,in}$	2.5	0.8	0.8	0.8	0.8	0.8
R_N	0.8	0.4	0.4	0.4	0.4	0.4
R_{SC}	0.8	6.5	6.5	6.5	6.5	6.5
R_{Com}	0	2.14	2.5	2.5	2.5	2.5
R_T	0.8	0.8	0.8	0.8	0.8	0.8
R_{diff}	2.5	2.14	2.5	2.5	2.5	2.5
l_{in}	0	2.5	2.5	2.5	2.5	2.5
l_{GN}	2.5	0	0	0	0	0
l_{SC}	2.5	5.26	5.26	5.26	5.26	5.26
l_{Con}	0	12.5	8	8	8	8
l_{MT}	2.5	5	0	6.4	12.8	13.2
l_{diff}	12.5	12.5	20	20	20	21.2
Θ_N	7.74	25	25	25	25	25
Θ_{Con}	0	6.11	11.9	11.9	11.9	11.9
Θ_{diff}	7.74	6.11	11.9	11.9	11.9	11.9
D_{GN}	0.26	0.26	0.26	0.26	0.26	0.26

Table 3: Number of grid points and average cell area for grid independent mesh

Ejector	Number of Grid Points	Average Cell Area (m^2)
Ejector A	151000	8.0E-08
Ejector B	136000	1.0E-07
Ejector C	105000	1.3E-07
Ejector C1	168000	8.6E-08
Ejector C2	198000	7.6E-08
Ejector OG	201000	7.5E-08

Table 4: Value of parameter κ at which gas induction was fitted to experimental values at different geometric parameters

Ejector	L_{MT}/D_{MT}	D_N/D_{MT}	**Parameter (κ) Value**
C	0	$8/16$	1
C1	4	$8/16$	0.55
C2	8	$8/16$	0.325
A	8	$5/16$	4.125
A	8	$8/16$	0.75
A	8	$10/16$	0.9
B	3.2	$5/16$	2.2
B	3.2	$8/16$	0.4
B	3.2	$10/16$	4.8
C	0	$5/16$	5.5
C	0	$8/16$	1
C	0	$10/16$	1.2